Proceedings of the 10th Brazilian Congress of Thermal Sciences and Engineering -- ENCIT 2004
Braz. Soc. of Mechanical Sciences and Engineering -- ABCM, Rio de Janeiro, Brazil, Nov. 29 -- Dec. 03, 2004

Paper CIT04-0394

TRANSITION TO TURBULENCE IN A STABLE STRATIFIED TEMPORAL MIXING LAYER THROUGH DIRECT NUMERICAL SIMULATION

Denise Maria Varella Martinez
Departamento de Matemática, Fundação Universidade Federal do Rio Grande - FURG
PPGRHSA – IPH - Universidade Federal do Rio Grande do Sul – Av. Bento Gonçalves, 9500 – 91501-970
Porto Alegre – RS – Brazil
denise@ppgiph.ufrgs.br - denisevmartinez@yahoo.com.br

Edith Beatriz Camaño Schettini
Instituto de Pesquisas Hidraulicas, Universidade Federal do Rio Grande do Sul – Av. Bento Gonçalves, 9500 – 91501-970
Porto Alegre – RS – Brazil
bcamano@iph.ufrgs.br

Jorge Hugo Silvestrini
Departamento de Engenharia Mecânica e Mecatrônica, Pontifícia Universidade Católica do Rio Grande do Sul – Av. Ipiranga, 6681
90619-900 – Porto Alegre – RS – Brazil
jorgehs@em.pucrs.br

Abstract. *Shear and stable stratification are important features of turbulent flow in geophysical, environmental, and engineering applications. Nutrients, pollutants, or reactants present in these flows are transported and mixed by turbulent motion. The dynamics of stably stratified mixing layer is controlled by a competition between the vertical shear of the base flow and buoyancy forces due to ambient density stratification. The buoyancy effects acts reducing the growth rate of perturbation and delaying the transition to turbulence, while the shear supplies kinetic energy. The early stage of the transition mechanism of a stably stratified mixing layer occurs initially with the development of the Kelvin-Helmholtz (KH) instability. In this study, we examine the influence of stable stratification in the development of the KH instability by means of the direct numerical simulation (DNS), assuming the Boussinesq approximation. The set of simulations includes runs with different Richardson number. The two-dimensional simulations show that higher stratification inhibits the pairing process, reduces the exchange of energy between the KH vortices and the mean flow, limits the maximum KH wave amplitude and reduces the buoyancy flux. A simulation, for high Reynolds number, to identify the secondary instability of the KH type was done.*

Keywords*: Stable stratification, Kelvin-Helmholtz instability, direct numerical simulation, mixing layer, transition.*

1. Introduction

The dynamics of the stably stratified mixing layer, mainly its transition to turbulence, is a problem of considerable interest in fluid dynamics with applications in both geophysical sciences and engineering. This dynamics is controlled by a competition between the vertical shear of the base flow and buoyancy forces due to ambient density stratification. The buoyancy effects act reducing the growth rate of perturbation and delaying the transition to turbulence, while the shear supplies kinetic energy.

The stably stratified mixing layer develops at the interface of two parallel streams of fluid moving horizontally at different velocities and having different densities, the upper stream being lighter than the lower one. It is characterized by the formation of big spiral vortices resulting from a Kelvin–Helmholtz (KH) instability type, the early stage of the transition mechanism. The instability is due to the inflectional nature of the velocity profile; the vortex sheet initially created is linearly unstable and rolls up to form the coherent vortices.

Miles (1961) and Howard (1961), based on linear stability analysis, showed that to occur KH instability in stratified shear flow from an infinitely small disturbance, the Richardson number should be less than 0.25 somewhere within the flow. Numerical calculations of Hazel (1972) solve the linear stability equation with hyperbolic tangent profiles for velocity and density of equal thickness, corroborating Miles' results.

The transition mechanism of a stably stratified mixing layer in laboratory experiments was studied by Thorpe (1973), Koop et al. (1979) and Atsavapranee et al. (1997). They analyzed all stages of flow dynamics, from the growth of perturbation (KH instability, secondary shear instability in the braid region) to developed turbulence. These works attested that the effect of buoyancy forces is to reduce the kinetic energy and vertical turbulent transport.

In many experimental studies, the thickness of the initial velocity profile exceeds the thickness of the initial density profile by at least a factor two (Koop et al., 1979; Strang et al., 2001). In this case, and when Richardson number is larger than 0.07, a dispersive instability, called Holmboe instability, dominates the earlier flow dynamics (the KH instability being prevalent for $R_i \leq 0.07$) (Lawrence et al., 1991). We shall not consider this case in the present study.

The main objective of the current work is to analyze the influence of stable stratification on the development of KH instability. We use two-dimensional direct numerical simulations of the Navier-Stokes equations in the Boussinesq approximation, so that variations in density are sufficiently small compared to some reference value. Direct numerical simulations (DNS) are excellent instruments for investigation of the dynamics of stable mixing layer, since they solve

entirely all the spatial and temporal scales of the flow. The set of simulations includes runs with different Richardson number. Temporal variation of kinetic energy and mixing are analyzed and discussed.

2.Mathematical model and numerical method

The temporal mixing layer with periodic boundary conditions in the x-direction, and free-slip boundary condition in the z-direction is considered. We assume that the fluid motion is described by the Navier-Stokes equations using the Boussinesq approximation, in a Cartesian frame of reference $\Re$=(0;x,z),

$$\frac{\partial \mathbf{u}}{\partial t} + (\mathbf{u}.\nabla)\mathbf{u} = -\nabla p - R_i \rho \mathbf{i_z} + \frac{1}{R_e}\nabla^2 \mathbf{u} \tag{1}$$

$$\frac{\partial \rho}{\partial t} + (\mathbf{u}.\nabla)\rho = \frac{1}{P_r R_e}\nabla^2 \rho \tag{2}$$

$$\nabla.\mathbf{u} = 0 \tag{3}$$

where $\rho(x, z, t)$ is density or active scalar, $\boldsymbol{u}(x, z, t)$ is the velocity field, $p(x, z, t)$ is the pressure field. There are two non-dimensional relevant parameters; the Reynolds number $R_e = U\delta_i / \nu$ (based on the half velocity difference across the shear layer and on the initial vorticity thickness, defined by $\delta_i = 2U /(du/dz)_{max}$) and the Richardson number $R_i = g\Delta\rho R\delta_i / \rho_0 U^2$ (where $\Delta\rho R$ is density scale and R is the ratio of initial vorticity thickness to the density thickness). Here the thickness of the initial velocity profile is approximately 80% of the thickness of the initial density profile. The time is made dimensionless using the advective scale δ_i / U. We chose the units of length, velocity and density such that δ_i= 1, U =1 and $\Delta\rho$ = 1/R. In this manner, $R_e = 1/\nu$ and $R_i = g/\rho_0$. At $t = 0$, $\rho(x, z, t=0) = \rho_0 + \rho(z)$, where ρ_0 is a constant density reference and $\rho(z)$ is the basic density profile. In the present case, no density fluctuation is superposed upon $\rho(z)$ at $t = 0$. The initial profiles of velocity and density are

$$u(z, t=0) = U\, erf\left(\frac{\sqrt{\pi}\, z}{\delta_i}\right) \tag{4}$$

$$\rho(z, t=0) = -\frac{1}{R} erf\left(\frac{\sqrt{\pi}\, z R}{\delta_i}\right) \tag{5}$$

A two-dimensional sinusoidal perturbation is superimposed upon the basic velocity profile. This perturbation is composed by two waves corresponding to the most amplified wave number α_a and its firth sub-harmonic $\alpha_a/2$. The associated most unstable wavelength given by linear stability theory is approximately $\lambda_a = 7\delta_i$ (the most amplified wave number $\alpha_a = 2\pi/\lambda_a$ being $0.889\delta_i^{-1}$ (Michalke, 1964)). These perturbations promote, respectively, the development of the KH instability and vortex pairing. In such case, the side of computational domain is taken equal to $L_N = 7N\delta_i$ in order to obtain N vortices in the streamwise direction.

Equations (1-3) are solved numerically using a sixth-order compact finite difference scheme (Lele, 1992) to compute the spatial derivatives, while the time integration is performed with a third-order low-storage Runge-Kutta method (Williamson, 1980). The incompressibility condition (Eq. (3)) is ensured with a fractional step method via resolution of a Poisson equation for the pressure. More details about the numerical code can be found in Lardeau et al. (2002) and Silvestrini et al. (2002).

3. Code validation – Amplification rate

In order to validate the numerical code the evolution of a small sinusoidal disturbance was considered. The results were compared with linear stability theory, where the disturbance is described by the Taylor-Goldstein equation. This equation represents the Boussinesq approximation of the Rayleigh equation (that is, including vertical density stratification (Hazel, 1972)).

Firstly, the computational domain is a square of side $L=7\delta_i$, corresponding to the most amplified wave number $\alpha_a=0.889\delta_i^{-1}$ given by linear stability theory. The resolution is $7\delta_i/128$, the Reynolds number is 300, the Prandtl number is 1, and the Richardson number tested are 0, 0.1 and 0.2. As the size domain is $7\delta_i$ only the development of single KH billow happens, excluding the possibility of pairing. Here the vertical diffusion term, correspondent to streamwise velocity, was canceled. This diffusion increases the width of the shear layer during the simulation and implies a variation in time of the base flow, inducing variation of the amplification rate (Medeiros et al., 2002). The initial amplitude of the

perturbation was 10^{-6} U. Tests with different computational grid of $n_x \times n_z$ points (N1= 64 × 65; N2 = 64 ×129; N3 = 128 × 129) were done. As it is hoped, the grid size has a great influence over the amplification rate. The test with computational grid N1 does not confirm the theory. In test with grid N2 it was noticed that the longitudinal resolution interferes in the evolution of wave amplitude (case stratified), leading to the increase of the amplification rate (see Tab. 1).

Figure (1) shows the time evolution of the amplitude with different Richardson number (0; 0.1; 0.2) obtained from the simulation with grid N3. Clearly there is a region of exponential amplification, which corresponds to regime governed by the linear theory.

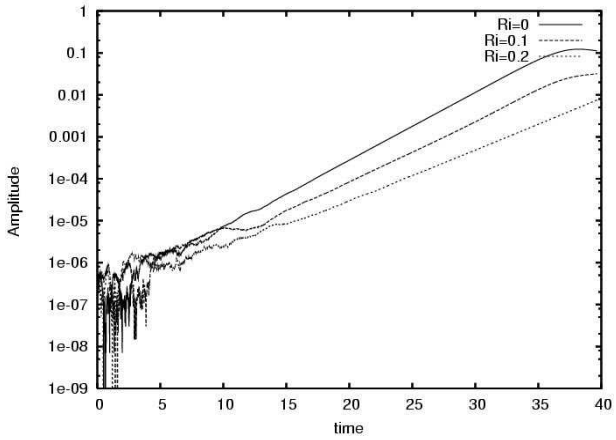

Figure 1. Amplitude evolution. Simulation N3.

Table 1 – Comparison of amplification rate with reference value (Hazel, 1972))

	Amplification rate			
R_i	N1 64 × 65	N2 64 × 129	N3 128 × 129	Ref. value
0	0.2254	0.1916	0.1861	0.1897
0.1	0.1682	0.2221	0.1650	0.1594
0.2	0.1441	0.1661	0.1388	0.1259

Comparison of the simulation N3 with the numerical results of Hazel (1972), shown in Tab.1, gives some accord for stably stratified mixing layer temporal growth rates, for R_i=0 and 0.1 while for R_i=0.2, a finest grid seems needed.

Hazel (1972), showed that the presence of boundaries makes longer waves more susceptible to instabilities, but the boundary effects are negligible when the total height of the fluid column H is large compared to the shear layer thickness, $H > 5\delta_i$ (Lawrence et al., 1991), which is a condition satisfied in our simulations.

4. Effects of the stable stratification

In following sections, the results from three simulations are presented. The parameters are summarized in Tab. (2). The amplitude of the perturbation superimposed upon the basic velocity profile, for the fundamental and the subharmonic mode, is showed in last column of the Tab. (2).

Table 2 – Parameters of two-dimensional simulations

Simulation number	R_e	R_i	Domain $L_x \times L_z$	Grid $n_x \times n_z$	Amplitude of perturbation
I	300	0; 0.1; 0.2	$14\delta_i \times 14\delta_i$	256 × 257	(1%U, 0.1%U)
II	300	0; 0.1; 0.2	$28\delta_i \times 14\delta_i$	256 ×257	(1%U, 0.1%U)
III	2000	0.167	$7\delta_i \times 7\delta_i$	768 × 961	(1%U, 0)

4.1. Two-dimensional visualizations

Firstly, the evolution of the unstratified mixing layer that is without buoyancy effect is analyzed. This flow manifests the typical dynamics: the growth of the most-amplified wavelength of the perturbations and the distortion into nonlinearity; the roll-up of the vorticity interface into Kelvin-Helmholtz vortices; the pairing of the large-scale structures and turbulent transition. These results are showed in Fig.(2) for three typical times. The initial vorticity, which is modulated by a small perturbation, progressively accumulates in the cores of KH vortices (Fig. 2a and Fig. 2b). These

cores are unstable to perturbation of wavenumber equal $\alpha_a/2$. The growth of this subharmonic perturbation leads to the pairing of the two vortices, Fig. (2c).

The primary KH vortices are not totally isolated from each other, but rather are connected by a thin braid of spanwise vorticity. In a stably stratified shear layer, these thin vorticity layers are strained in between the KH vortices, and intensified by buoyancy effects (Staquet. 1995; Caufield et al., 2000). The evolution of stable stratified mixing layer is conducted in order to investigate the stability of these layers.

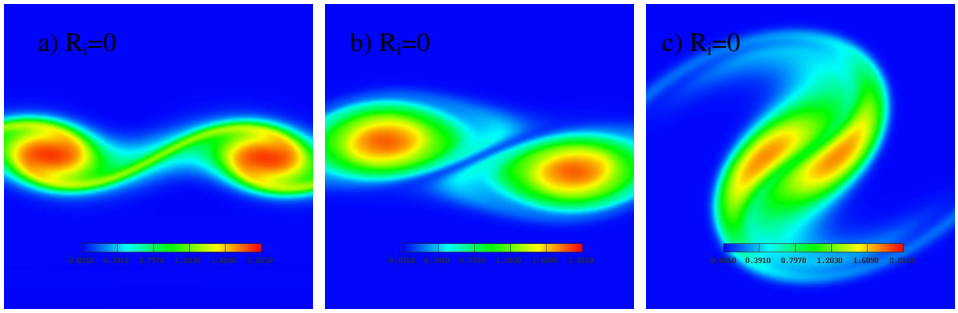

Figure 2. Spanwise vorticity field in an unstratified mixing layer. Simulation I, R_i =0, at time;
a) t = 9.52 δ_i/U; *b)* t =19.03 δ_i/U; *c)* t =28.55 δ_i/U;

The development of the KH instability on the stably stratified mixing layer produces a streamwise density gradient in the braids. This streamwise density gradient (corresponding to the spanwise component of the baroclinic torque, in the Boussinesq approximation) feeds the braid with vorticity and forms the baroclinic layer, an important local effect of buoyancy. The component of the baroclinic torque along the spanwise direction is below showed in the vorticity equation,

$$\frac{\partial \omega}{\partial t} + u\frac{\partial \omega}{\partial x} + w\frac{\partial \omega}{\partial z} = R_i \frac{\partial \rho}{\partial x} + \frac{1}{R_e}\left(\frac{\partial^2 \omega}{\partial x^2} + \frac{\partial^2 \omega}{\partial z^2}\right) \tag{6}$$

The generation of vorticity is due to the fact that is a variation in the density field rather than a gradient in the velocity, the only generation possible is in the plane perpendicular to the line marking the stratification (Criminale et. al. ,2003).

It follows that vorticity can locally increase beyond its maximum value for the stratified case. This property yields a different behavior of the stratified mixing layer as opposed to its unstratified counterpart. The baroclinic layer forms under the action of buoyancy effects and strains between the KH vortices. During the roll-up, heavy and light fluid are brought together from the outer side of the mixing layer towards the center of the mixing layer, yielding a strong density gradient there. This baroclinic layer is observed in our simulations. Figure (3) and Fig. (4) show that increasing Richardson number inhibits the pairing process and the braid vorticity exceeds the cores' one.

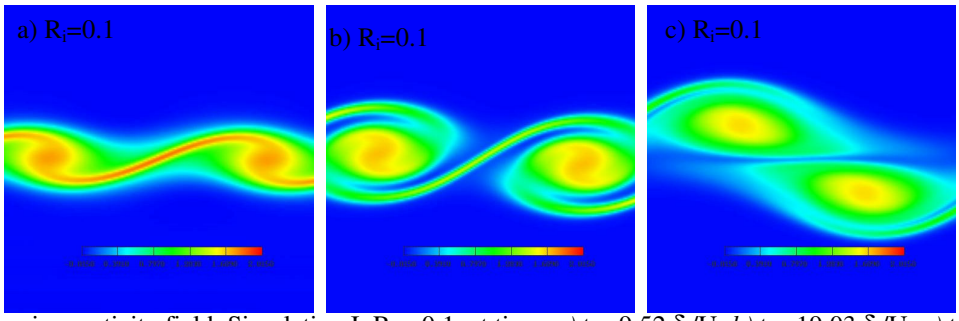

Figure 3. Spanwise vorticity field. Simulation I, R_i = 0.1, at time; a*)* t = 9.52 δ_i/U; *b)* t = 19.03 δ_i/U; *c)* t = 28.55 δ_i/U;

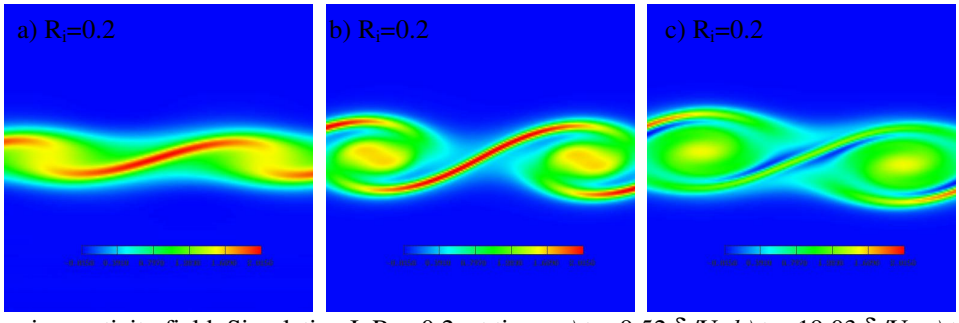

Figure 4. Spanwise vorticity field. Simulation I, R_i = 0.2, at time; *a)* t = 9.52 δ_i/U; *b)* t = 19.03 δ_i/U; *c)* t = 28.55 δ_i/U;

Also is observed that there is a decrease of the thickness of mixing layer, this is why stratified flows required finer grids than unstratified flows. The stable stratification and baroclinic effect, through streamwise variations of the density field, weakens the vertical motions.

Therefore, the stable stratification has a stabilizing effect on the growth of the primary KH instability, resulting in a decrease of overall fluid entrainment and reducing the mixing process.

With the growth of the instability appears a vortex between two stretched vorticity layers, showed in Fig (3a) and Fig.(4a-b). These layers are also regions of strong streamwise density gradients.

Figure (5) shows the development of Kelvin-Helmholtz instability in simulation II. In the unstratified case, R_i=0, it is observed that the vorticity is dissipated by viscosity in the braids. When the KH vortex achieves its maximum energy and pairs, the vorticity remaining in the core is substantially greater than that in the braids. On the contrary, when the stratification is higher (Ri =0.2) the vorticity is increased in the braids and the baroclinic layer is visible.

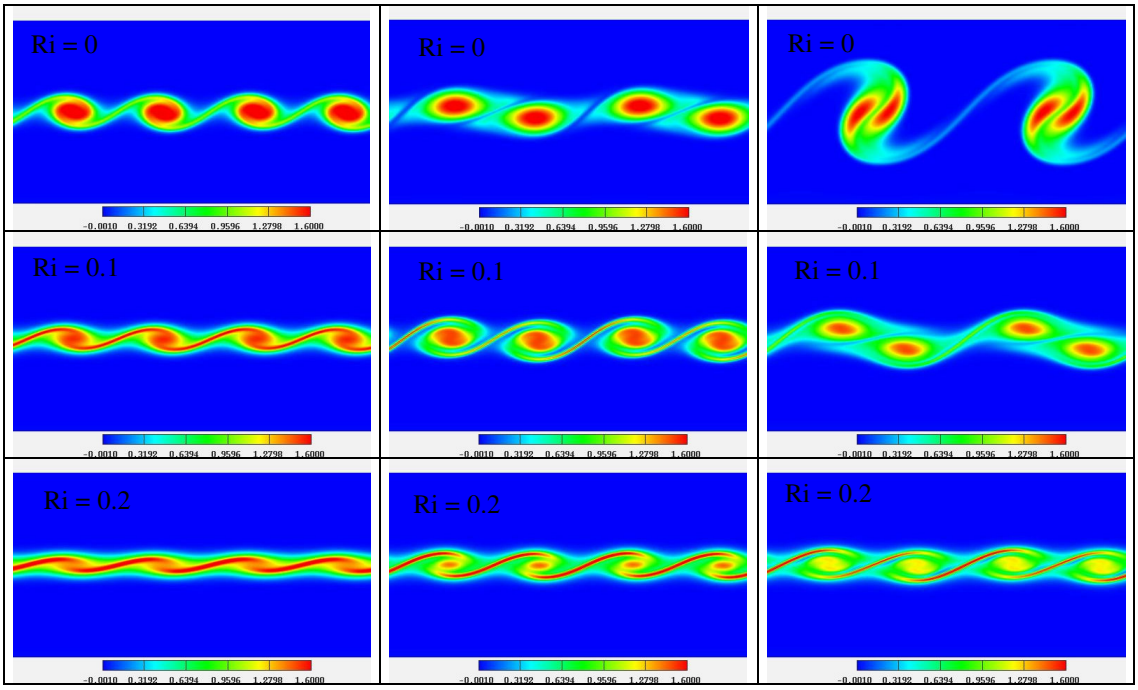

Figure 5. Vorticity fields in times t =14.27 δ_i/U; t = 23.79 δ_i/U; t = 33.3 δ_i/U (left to right)

Figure (6) illustrates the density field for different Richardson numbers at same time (simulation I). It shows that process of roll-up of the KH billow also strongly modifies the density distribution.

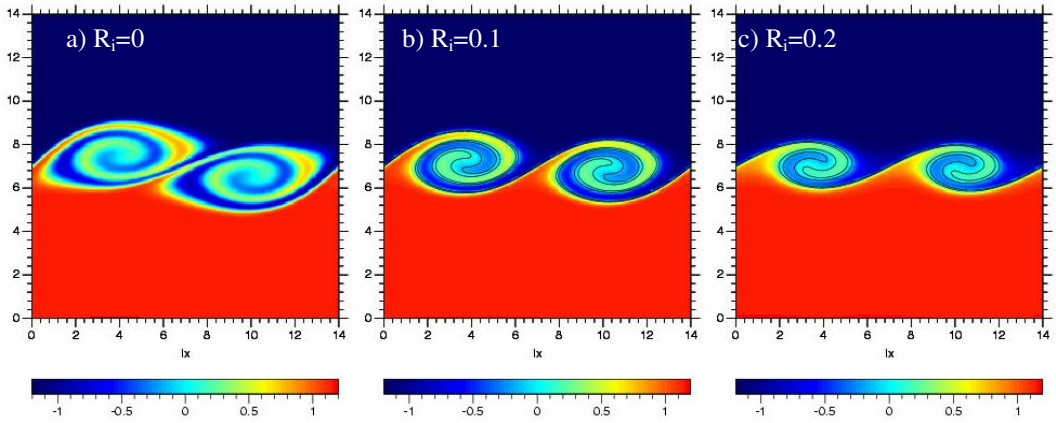

Figure 6. Density field at time tU/δ_i =19.03.

4. 2. Kinetic Energy

To quantify the effect that stable stratification (buoyancy forces) has on the development of KH instability we make use of the time evolution of the kinetic energy. Following Klaassen et al. (1991), if (u, w) represents the instantaneous velocity vector of the non linear KH wave, then the kinetic energy per unit horizontal area is given by

$$K = \frac{1}{2L}\int_0^L\int_0^L \left(\left(u - \langle u \rangle\right)^2 + w^2 \right) dxdz \tag{7}$$

where the ensemble average of the streamwise velocity is $\langle u \rangle = \frac{1}{L}\int_0^L u\,dx$. Figure (7) shows the evolution of the kinetic energy *K* for different Richardson numbers. In simulation number I the maximum kinetic energy is attained when the KH vortices pairs, in (Fig. (7a) and (2c)). When four vortices are simulated (Fig. (7b)) the peak of the maximum kinetic energy is considered for the first pairing (unstratified and stratified cases), then it oscillates and increases near the second pairing for the unstratified case.

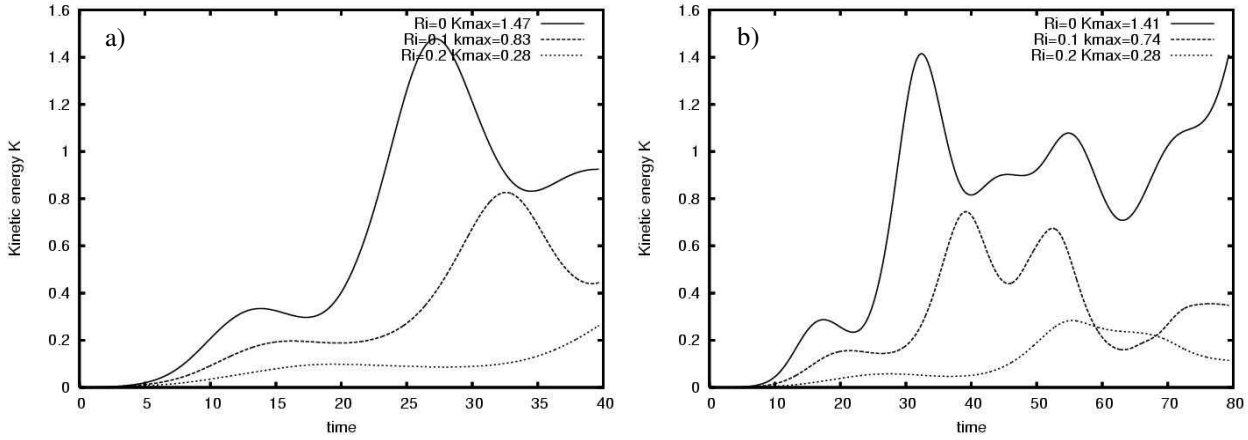

Figure 7. The effect of the bulk Richardson number on the evolution of wave Kinetic energy (*K*), R_e=300. a) Two vortices; b) Four vortices.

It seems clear from Fig. (7) that the maximum KH vortices amplitude is limited by the presence of strong stable stratification (Ri ≥ 0.1) in the flow and that the time at which maximum *K* is reached, is considerably delayed when the stratification is increased. These characteristics are consistent with the expectation that the wave needs to execute work against the gravitational potential in order to grow. The data indicates that when Richardson number increases, the amplitude of the oscillations decreases and the peak of maximum *K* is retarded. This may be associated with an exchange of energy between the KH vortices and the flow.

4. 3. Mean density field and buoyancy flux

Measurements of the time evolution of mean density field $\langle \rho \rangle$ and buoyancy flux $\langle \rho' w' \rangle$ are show in Fig. (8). These two quantities play a fundamental role in the dynamics of stratified flows, since mixing and growing of the layer depend on them.

The buoyancy flux is defined as $F = \langle \rho' w' \rangle$, where ρ' and w' are the fluctuations of density and vertical velocity, and the < > denotes of average on the streamwise direction (Hug et al., 1995).

The spreading of the buoyancy flux $\langle \rho' w' \rangle$ is due to the buoyancy effects (Fig. (8e) and (8f)). In the unstratified case, there are no buoyancy effects and the density is a perfect passive scalar (Fig.(8d)). At time t = 19.03 δ_i/U, the vortices are dislocated in relation to the z-center the domain (Fig. 2b), producing negative values of the $\langle \rho' w' \rangle$. Figure (8e) and Fig. (8f) show that there is a strong decrease of the buoyancy flux caused by reduction of the fluctuations of vertical velocity. This drastic reduction of the buoyancy flux as Richardson number increases is also caused by a combination of the reduction of volume fluid entrainment into KH vortices, and delaying process of pairing of the large structures. For the higher Richardson number, the gravity plays a dominant effect. In these cases, for the KH vortices win the stratification effect, it is necessary to develop an important work against the gravitational potential. The average density profile is very different between Fig. (8a), (8b) and (8c) because, as cited above, there is a decrease of the thickness of mixing layer due to baroclinic effects that weaken the vertical motions. Therefore, the vertical size of the vortex is larger in unstratified than in the two stratified cases.

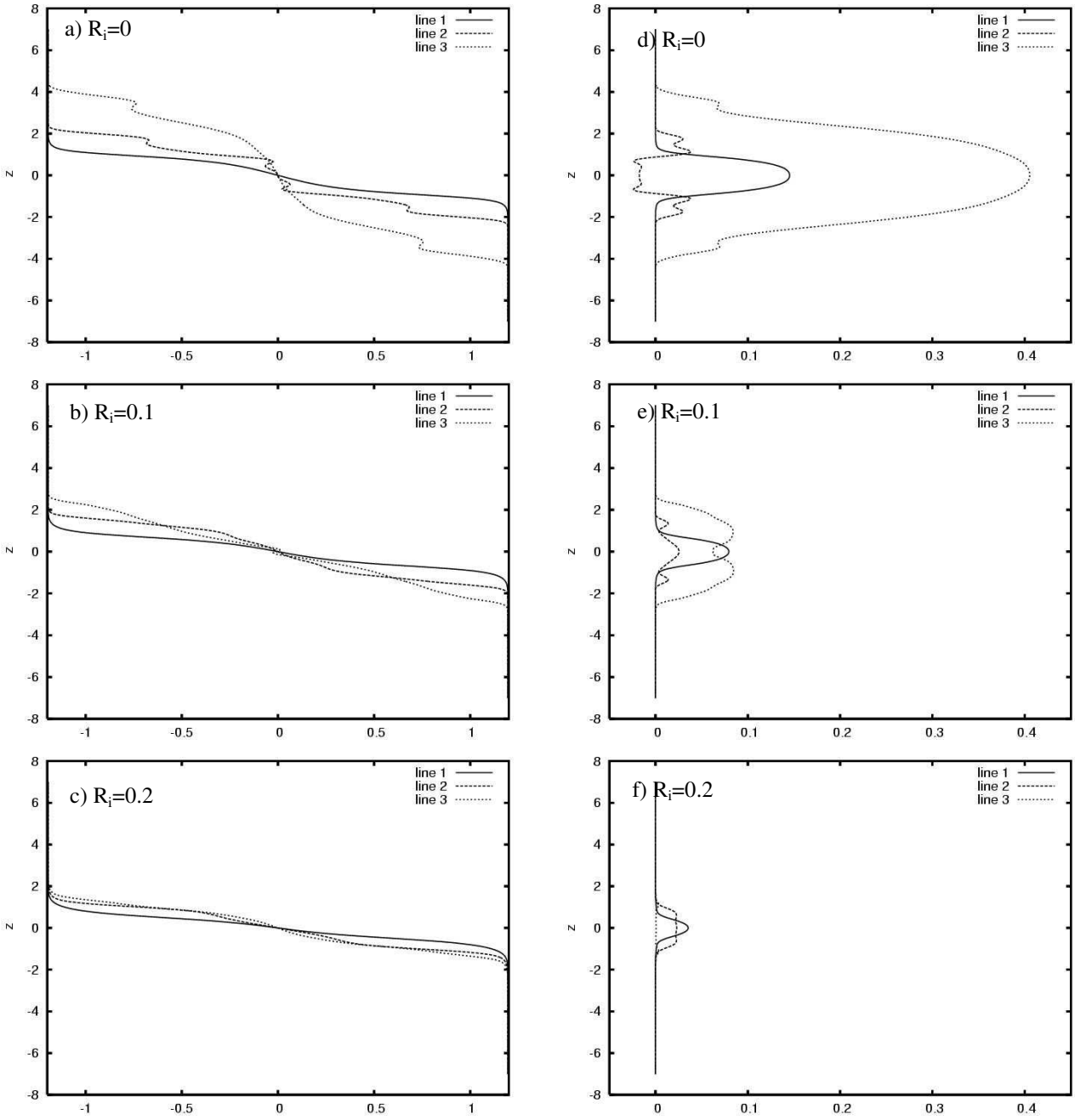

Figure 8. (a –c) Mean density profile $\langle \rho \rangle$; (d – f) Buoyancy flux $\langle \rho' w' \rangle$; Simulation I.
Line 1– t = 9.52 δ_i/U; line 2 – t =19.03 δ_i/U; line 3 – t =28.55 δ_i/U

5. Secondary instabilities in two-dimensional baroclinic layer

As cited above, the baroclinic layer does not exist in an unstratified flow. This baroclinic layer may be subjected to secondary instabilities, when the fluid is strongly stratified and for higher Reynolds numbers. In laboratory experiments done by Atsavapranee et al. (1997), it could be observed small KH type vortical structures between two primary vortices. The presence of the secondary shear instability in a stratified mixing layer is due to baroclinic vorticity generation in the stratified flow (see Eq. (6)).

Following Staquet (1995), a secondary instability starts developing in the baroclinic layer, with one KH vortex, for $R_e \geq 1500$. She shows that these negative vorticity layers are generated by strong streamwise density gradients, and indirectly results from convective activity in the vortex core. Indeed, the production of negative vorticity in the vortex core is rapidly followed by the growth of the secondary instability. Moreover, this instability does not develop if negative vorticity is too low compared to the positive one.

The vorticity can locally increase beyond its maximum initial value, even if the flow dynamics is two-dimensional, and transfer of energy towards small scales, as in three-dimensional turbulence. It is the non-conservation that makes

possible the successive secondary instabilities (type KH), in enabling the existence of a baroclinic layer of higher leves of vorticity than the initial one, as well as the generation of zones of negative vorticity.

A simulation was done for Re = 2000 and Ri = 0.167(simulation III in Tab. 2). Figure (9) shows that the baroclinic layer develops a secondary instability along the braid due to the concentration of vorticity. These instabilities yield coherent structures which are very similar in appearance and dynamics to the primary KH vortices, except for the smaller size (Fig. (9b-d)).

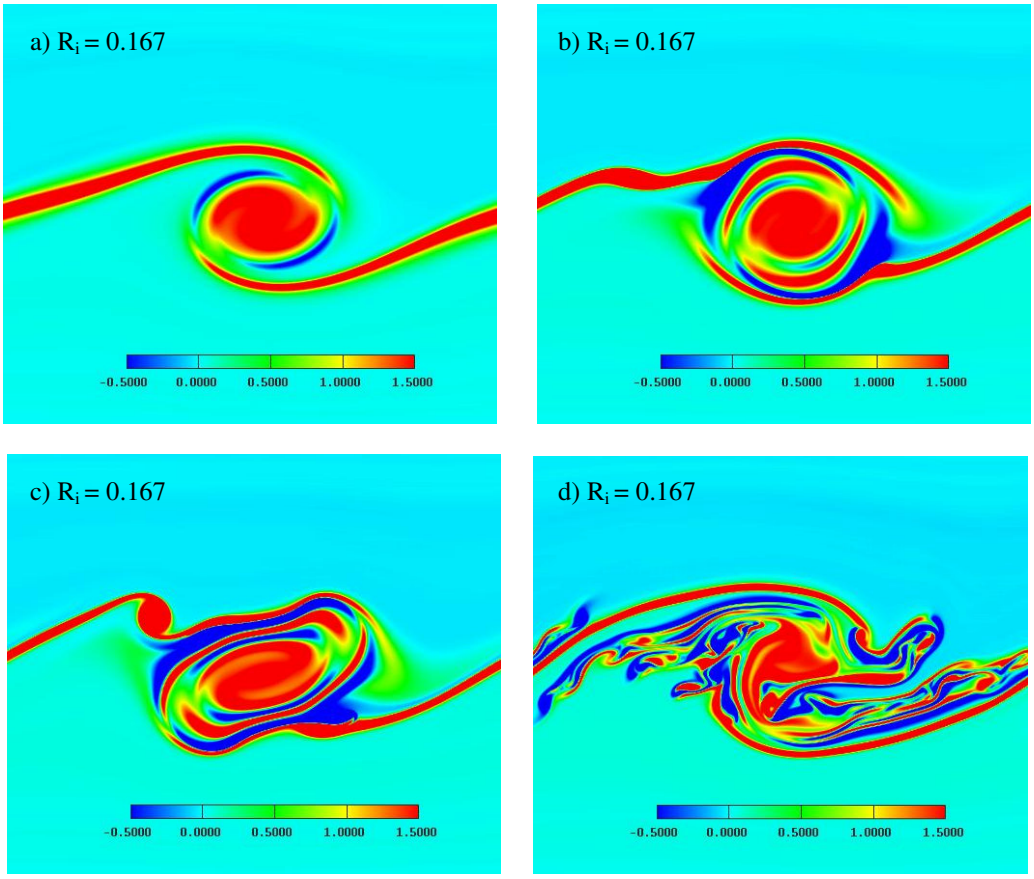

Figure 9. Development of secondary instabilities in a mixing layer, Re=2000, R_i =0.167.

The occurrence of secondary instabilities in tri-dimensional case is still a matter of discussion. We intend to investigate how these instabilities compete with the 3D instabilities and hence verify the occurrence of the KH type secondary instabilities in a tri-dimensional case.

6. Conclusions

The purpose of the present study was to investigate numerically the effect of the stable stratification (buoyancy forces) on the development of KH instability. The two-dimensional simulations showed that higher stratification increasingly inhibits the pairing process, reducing the exchange of energy between the KH vortices and the flow, limits the maximum KH wave amplitude and reduces the buoyancy flux.

In the two-dimensional mixing layer, the pairing process (Fig. 2c and Fig. 6) was found to play a critical role in the mixing transition and govern the growth of the mixing layer.

In this work, we presented the variations of buoyancy flux with stratification and the appearance of the secondary instability in the baroclinic layer when Re = 2000. The secondary stability, of the KH type, develops at the stagnation point of the baroclinic layer, for Re ≥ 2000, when only one primary KH vortex develops in the flow.

7 Acknowledgement

The authors wish to thank the Coordenação de Aperfeiçoamento de Pessoal de Nível Superior – CAPES for sponsoring this project.

8. References

Atsavapranee, P. and Gharib, M., 1997, “Strutures in Stratified Plane Mixing Layers and the Effects of Cross-shear”, J. Fluid Mech., Vol. 342, pp. 53-86.

Caufield, C. P. and Peltier, W. R., 2000, "The Anatomy of the Mixing Transition in Homogeneous and Stratified Free Shear Layers", J. Fluid Mech., Vol. 413, pp. 1-47.

Criminale, T. L. J. and Joslin, R., 2003, "Theory and Computational Hydrodynamic Stability", Cambridge University Press.

Hazel, P., 1972, "Numerical Studies of the Stability of Inviscid Stratified Shear Flows", J. Fluid Mech., Vol. 51, part. 1, pp. 39-61.

Howard, L. N., 1961, Note on a paper of John W. Miles, J. Fluid Mech., Vol.10, pp. 509- 512.

Huq, P. and Britter, R. E., 1995, "Turbulence Evolution and Mixing in a Two-layer Stably Stratified Fluid", J. Fluid Mech., Vol. 285, pp. 41-67.

Klaaseen, G. P. and Peltier, W. R., 1991, "The Influence of Stratification on Secondary Instability in Free Shear Layers", J. Fluid Mech., Vol. 227, pp. 71-106.

Koop, C. G. and Browand, F. K., 1979, "Instability and Turbulence in a Stratified Fluid with Shear", J. Fluid Mech., Vol. 93, part 1, pp. 135-159.

Lardeau, S., Lamballais, E. and Bonnet, J. P., 2002, "Direct Numerical Simulations of a Jet Controlled by Fluid Injection", J. Turbulence. Vol.3 002

Lawrence, G. A., Browand, F. K. and Redekopp, L. G., 1991, "The Stability of a Sheared Density Interface", Phys. Fluids A, Vol. 3, pp. 2360-2370.

Lele, S. K., 1992, "Compact Finite Difference Schemes with Spectral-like Resolution", J. Comput. Phys., Vol. 103, pp. 16-42.

Medeiros, M. A. F., Silvestrini, J. H. and Mendonça, M. T., 2002, "Using Linear and Non Linear Stability Theory for Evaluating Code Accuracy", Proceedings of the III Escola de Primavera em Transição e Turbulência, Florianópolis, Brazil.

Miles, J. W., 1961, "On the stability of Heterogeneous Shear Flows", J. Fluid Mech., Vol.10, pp. 496 -508.

Michalke, A., 1964, "On the Inviscid Instability of the Hyberbolic-tangent Velocity Profile", J. Fluid Mech.,Vol. 19, pp. 543-556.

Silvestrini, J. H., Lamballais, E., 2002, "Direct Numerical Simulation of Wakes with Virtual Cylinders", Int. J. of Computational Fluid Dynamics, Vol.16 (4), pp. 305 – 314.

Staquet, C., 1995, "Two-dimensional Secondary Instabilities in a Strongly Stratified Shear Layer", J. Fluid Mech.,Vol. 296, pp. 73-126.

Strang, E. J. and Fernando, H. J. S., 2001, "Entrainment and Mixing in Stratified Shear Flows", J. Fluid Mech., Vol. 428, pp. 349-386.

Thorpe, S. A., 1973, "Experiments on Instability and Turbulence in a Stratified Shear Flow", J. Fluid Mech., Vol. 61, part 4, pp. 731-751.

Williamson, J. H., 1980, " Low-storage Runge-Kutta Schemes", J. Comput. Phys., Vol. 35, pp. 48-56.